Postnatal Chick Choroids Exhibit Increased Retinaldehyde Dehydrogenase Activity During Recovery From Form Deprivation Induced Myopia

Angelica R. Harper,[1] Xiang Wang,[1] Gennadiy Moiseyev,[2] Jian-Xing Ma,[2] and Jody A. Summers[1]

[1]Department of Cell Biology, University of Oklahoma Health Sciences Center, Oklahoma City, Oklahoma, United States
[2]Department of Physiology, University of Oklahoma Health Sciences Center, Oklahoma City, Oklahoma, United States

Correspondence: Angelica R. Harper, Department of Cell Biology, University of Oklahoma Health Science Center, BRC, Room 266, 975 NE 10th Street, Oklahoma City, Oklahoma 73104, USA; angelica-harper@ouhsc.edu.

Submitted: February 19, 2016
Accepted: June 30, 2016

Citation: Harper AR, Wang X, Moiseyev G, Ma J-X, Summers JA. Postnatal chick choroids exhibit increased retinaldehyde dehydrogenase activity during recovery from form deprivation induced myopia. *Invest Ophthalmol Vis Sci*. 2016;57:4886–4897. DOI: 10.1167/iovs.16-19395

Purpose. Increases in retinaldehyde dehydrogenase 2 (*RALDH2*) transcript in the chick choroid suggest that RALDH2 may be responsible for increases observed in all-trans-retinoic acid (atRA) synthesis during recovery from myopic defocus. The purpose of the present study was to examine RALDH2 protein expression, RALDH activity, and distribution of RALDH2 cells in control and recovering chick ocular tissues.

Methods. Myopia was induced in White Leghorn chicks for 10 days, followed by up to 15 days of unrestricted vision (recovery). Expression of RALDH isoforms in chick ocular tissues was evaluated by Western blot. Catalytic activity of RALDH was measured in choroidal cytosol fractions using an in vitro atRA synthesis assay together with HPLC quantification of synthesized atRA. Distribution of RALDH2 cells throughout the choroid was evaluated by immunohistochemistry.

Results. RALDH2 was expressed predominately in the chick choroid ($P < 0.001$) and increased after 24 hours and 4 days of recovery (76%, 74%, and 165%, respectively; $P < 0.05$). Activity of RALDH was detected solely in the choroid and was elevated at 3 and 7 days of recovery compared to controls (70% and 48%, respectively; $P < 0.05$). The number of RALDH2 immunopositive cells in recovering choroids was increased at 24 hours and 4 to 15 days of recovery ($P < 0.05$) and were concentrated toward the RPE side compared to controls.

Conclusions. The results of this study suggest that RALDH2 is the major RALDH isoform in the chick choroid and is responsible for the increased RALDH activity seen during recovery.

Keywords: myopia, retinoic acid, choroid, RALDH2, form deprivation

Clinical and experimental evidence has indicated that postnatal ocular growth is regulated by a vision-dependent emmetropization process that coordinates growth of the ocular tissues, resulting in clear, uncorrected vision.[1,2] In humans, pathologic or environmental disturbances to the natural emmetropization process lead to abnormal elongation of the posterior portion of the eye and result in the development of myopia or nearsightedness.[1–4] Interruption of emmetropization in animal models, such as the chick, primate, and guinea pig, through the application of translucent occluders (form deprivation) causes a distortion in visual quality, which results in ocular growth and myopia through changes in the regulation of scleral extracellular matrix (ECM) remodeling.[5–9] Interestingly, form deprivation–induced myopia is reversible; removal of the occluder and subsequent detection of myopic defocus results in a rapid cessation of axial growth and the eventual reestablishment of emmetropia (recovery).[10]

While it generally is understood that visually guided ocular growth is regulated locally via a retinal to scleral signaling cascade,[11–15] few molecules that have a direct effect on the regulation of scleral ECM remodeling and ocular growth have been identified. Recent studies in animal models implicate all-trans-retinoic acid (atRA) as a key signaling molecule in the regulation of postnatal ocular growth.[16–20] In the chick, choroidal atRA synthesis increases during recovery from deprivation-induced myopia and decreases during myopia development.[16,17] Moreover, atRA has been demonstrated to directly inhibit proteoglycan synthesis in the chick and primate sclera.[16–18] Therefore, atRA may represent a visually regulated chemical signal that can directly regulate ocular growth and refraction.

Synthesis of atRA occurs by two oxidation reactions: first, the oxidation of retinol to retinaldehyde by the retinol dehydrogenase (RDH) enzymes, RDH1, DHRS9, and RDH10,[21] and second, the oxidation of retinaldehyde to atRA by one of three retinaldehyde dehydrogenase (RALDH) enzymes: RALDH1, RALDH2, or RALDH3 (also known as ALDH1a1, ALDH1a2, and ALDH1a3). In a study examining transcriptional changes in response to imposed defocus, Simon et al.[22] determined that changes in choroidal *RALDH2* transcript is rapid and specific for the sign of defocus. In addition, we previously identified RALDH2 as the key RALDH isoform regulating atRA synthesis during recovery from visually-induced ocular growth in chicks.[17] Significant increases in choroidal *RALDH2* transcript were observed following 12 hours of recovery with transcript levels returning to control by 15 days. No changes were observed in *RALDH3* expression, and transcript levels of choroidal *RALDH1* were undetectable.

These results suggest that, in response to myopic defocus, the levels of choroidal RALDH2 increase which, in turn, increase the production of atRA. We speculate that choroidally generated atRA is transported to the sclera, where it decreases scleral proteoglycan synthesis, causing a deceleration in ocular growth rate. Therefore, the current investigation was done to extend our previous studies by examining RALDH2 protein expression and RALDH enzymatic activity in chick eyes in various growth states, and examining the changes in distribution of RALDH2-synthesizing cells in the choroid in response to myopic defocus.

Materials and Methods

Animals

White Leghorn male chicks (*Gallus gallus*) were obtained as 2-day-old hatchlings from Ideal Breeding Poultry Farms (Cameron, TX, USA). Chicks were housed in temperature-controlled brooders with a 12-hour light/dark cycle, and were given food and water ad libitum. Form deprivation myopia (FDM) was induced in 3-day-old chicks by applying translucent plastic goggles to one eye, as described previously.[9] The contralateral eyes (left eyes) of all chicks were never goggled and used as controls. Chicks were checked daily for the condition of the goggles. Goggles remained in place for 10 days, after which time the chicks were either euthanized for isolation of ocular tissues from control and form-deprived eyes (= time 0), or the goggles were removed and chicks were allowed to experience unrestricted vision (recover) for up to 15 days.

Chicks were managed in accordance with the ARVO Statement for the Use of Animals in Ophthalmic and Vision Research, with the Animal Welfare Act, and with the National Institutes of Health (NIH; Bethesda, MD, USA) Guidelines. All procedures were approved by the Institutional Animal Care and Use Committee of the University of Oklahoma Health Sciences Center.

Tissue Isolation and Preparation

To prepare ocular tissues for analysis, chicks were euthanized by an overdose of isoflurane inhalant anesthetic (IsoThesia; Vetus Animal Health, Rockville Center, NY, USA) at various time points during recovery, and eyes were enucleated. Eyes were cut along the equator to separate the anterior segment and posterior eye cup. Anterior tissues were discarded, and the vitreous body was removed from the posterior eye cups. An 8-mm punch was taken from the posterior pole of the chick eye using a dermal biopsy punch (Miltex, Inc., York, PA, USA). Punches were located nasal to the exit of the optic nerve, with care to exclude the optic nerve and pecten. In younger birds (ages 13–14 days), this punch represented approximately 85% of the posterior hemisphere, due to small eye size. Western blots and atRA synthesis assays were normalized to punch size as it is known that there is an increased vascular permeability and extravasation of serum proteins into the choroidal stroma during recovery.[23] With the aid of a dissecting microscope, the neural retina and RPE were isolated from the underlying choroid and sclera with a drop of PBS (3 mM dibasic sodium phosphate, 1.5 mM monobasic sodium phosphate, 150 mM NaCl, pH 7.2) and gentle brushing. Retina and RPE were pooled for each punch, placed in microfuge tubes, and stored on ice. Following removal of RPE, choroids were gently dissected from the sclera by placing a small, rounded spatula between the two tissue layers and carefully lifting the choroid off the sclera. Choroids and sclera then were placed into microfuge tubes on ice. Retina/RPEs, choroids, and sclera were stored at −20°C until time of use.

To prepare tissue homogenates, retina/RPEs and choroids were separately homogenized in RALDH homogenization buffer (20 mM triethanolamine-HCl pH 7.4, 1 mM dithiothreitol, 0.1 mM EDTA) using a VirTis rotor-stator homogenizer (SP Industries, Gardiner, NY, USA). Sclera were snap-frozen in liquid nitrogen, added to a dounce homogenizer (Micro-Metric Instruments, Tampa, FL, USA) containing 500 µL RALDH homogenization buffer and ground until most tissue was solubilized. Following a 500 µL rinse with homogenization buffer, sclera homogenates were homogenized further using a VirTis rotor-stator homogenizer (SP Industries). After homogenization, a maximum of 1.0 mL of each homogenate was placed in 1.5 mL tubes and centrifuged (12,000*g* for 20 seconds; Eppendorf Microfuge 5148, Hamburg, Germany) at 4°C to remove debris from the whole tissue homogenate. Homogenate was transferred to thick-walled microfuge tubes (polyallomer tubes; Beckman Coulter, Brea, CA, USA) and ultracentrifuged (100,000*g* for 1 hour; Optimum MAX Ultracentrifuge, Beckman Coulter) at 4°C to isolate microsomal fraction (pellet) and cytosol fraction (supernatant). Fractions were isolated and stored at −20°C. In some cases, protein concentrations of ocular tissue samples were determined by a Bradford assay (BioRad, Hercules, CA, USA).

Generation of Chick RALDH1, 2, and 3 Plasmids

Generation of the RALDH1, 2, and 3 plasmids was achieved as described previously for rat RALDH2.[24] However, differences in the chicken RALDH sequences necessitated the following modifications. Chick retina/RPE and choroid cDNA were generated from total RNA using random hexamers and reverse transcriptase, as described previously.[17] Chick retina/RPE cDNA was used as the template to amplify the full length coding sequence of RALDH1, whereas choroid cDNA was used to amplify the full length coding sequence of RALDH 2 and RALDH3 using gene specific primers designed with NdeI and XhoI restriction sites to flank the 5′ and 3′ ends of each RALDH construct, respectively (Table 1). Genes were amplified using 1X Phusion HF buffer (New England Biolabs, Ipswich, MA, USA), 200 µM each dNTP, 0.5 µM each primer, <250 ng template cDNA, 3% dimethyl sulfoxide (DMSO), and 1 unit of Phusion DNA polymerase (New England Biolabs) in a DNA thermal cycler (PerkinElmer, Waltham, MA, USA) using the following PCR conditions: 2 minutes at 95°C, 35 cycles of 1 minute at 95°C, 1 minute at 60°C, and 7 minutes at 72°C after the final cycle. Products of PCR were run on a 1.0% agarose gel, and the 1.5 kb products were gel purified using a QIAquick gel extraction kit (Qiagen, Limburg, Netherlands), according to manufacturer's protocol.

RALDH1, 2, and 3 cDNA was subcloned into the pJet 1.2/blunt Cloning Vector (Thermo Fisher Scientific, Waltham, MA, USA), according to the manufacturer's blunt-end cloning protocol. The plasmids were transformed into MAX Efficiency DH5α Competent Cells (Invitrogen, Grand Island, NY, USA), according to manufacturer's protocol with the following modifications: (1) only 50 µL of competent cells were used and (2) 1 to 3 µL of the ligation reaction was added to the competent cells. Following the incubation on ice and heat shock, 900 µL of S.O.C. medium was added to the cells, and cells were shaken at 13*g* and 37°C for 1 hour; 50 to 200 µL of the cells were plated on Luria Broth (LB), agarose plates with carbenicillin (100 µg/mL; Sigma-Aldrich Corp., St. Louis, MO, USA) selectivity, and plates were placed in a 37°C incubator overnight. Colonies were screened for the correct plasmid by colony PCR with PCR cycle conditions identical to those described above. Products of PCR then were run on a 1.0%

Investigative Ophthalmology & Visual Science

Table 1. Gene Primers*

Gene	Forward Primer	Reverse Primer
RALDH1	5′-CACACACATATGAAGAAGCAAGGCTCACCCAGC-3′	5′-CACACACTCGAGTTATGAGTTCTTCTGTGGGAT-3′
RALDH2	5′-CACACACATATGGCATCTCTGCATCTGCTGCCT-3′	5′-CACACACTCGAGTTAGGAATTCTTCTGAGGGAT-3′
RALDH3	5′-CACACACATATGGCCGCGGTCAACGGTGCTGTG-3′	5′-CCACACACTCGAGTCATGGACTCTTCTGGGACAG-3′

* NdeI restriction sites indicated with single underline. XhoI restriction sites indicated with double underline. Six base pairs added on 5′ end of each primer to assist digestion.

agarose gel to identify colonies positive for the RALDH plasmids. Positive colonies were removed gently from the plates, added to polypropylene round-bottomed tubes containing 3 mL LB and 100 μg/mL carbenicillin, and placed in a 37°C incubator shaker at 16*g* for 8 hours. 1.0 mL of each bacterial culture then was added to 1 L flasks containing 250 mL LB broth and 100 μg/mL carbenicillin, and flasks were placed in a 37°C incubator shaker at 16*g* overnight. RALDH1, 2, and 3 plasmids were purified using a Qiagen Plasmid Maxi kit according to manufacturer's protocol.

To isolate the RALDH1, 2, and 3 inserts from the pJet cloning vector, purified plasmids were double digested with NdeI and XhoI using 1 to 3 μg of RALDH/pJet plasmid. Plasmid, 60 units of NdeI, 60 units of XhoI, and 1× CutSmart buffer (New England Biolabs) in a 60 μL total reaction volume were incubated at 37°C overnight. The digests were run on a 1.0% agarose gel, and the approximately 1.5 kb inserts were gel purified using a QIAquick gel extraction kit (Qiagen), according to the manufacturer's protocol. In tandem, pET-15b vector (EMD/Millipore, Darmstadt, Germany) also was digested with NdeI and XhoI, as described above. The digest was run on a 1.0% agarose gel, and the linearized vector (5.7 kb) was gel purified. To prevent recircularization of the pET-15b vector, 2 to 3 μg of vector was dephosphorylated with 5 units of Antarctic Phosphatase (20 μL total reaction volume; New England Biolabs), according to the manufacturer's protocol. RALDH1, 2, and 3 inserts then were ligated into the dephosphorylated pET-15b vector in a 3:1 (insert to vector) ratio. Appropriate volumes of the respective insert and vector were added to a microfuge tube containing 400 units T4 DNA ligase (New England Biolabs) and 1X T4 DNA ligase reaction buffer (20 μL total reaction volume). Ligation reactions were incubated for 30 minutes at RT and then placed in a 65°C water bath for 10 minutes. One to 3 μL of each ligation reaction was used to transform MAX Efficiency DH5α Competent Cells (Invitrogen), as described above and plated on LB agarose plates with Carbenicillin selectivity (100 μg/mL; Sigma-Aldrich Corp.). Colony PCR, growth of bacterial cultures, and maxi preps were performed as described above. Nucleotide sequences of cloned RALDH constructs and plasmids was confirmed by DNA sequencing at each step of the cloning process (Oklahoma Medical Research Foundation DNA Sequencing Facility).

Expression and Purification of Chick RALDH1, 2, and 3 Protein

Expression and purification of the RALDH1, 2, and 3 proteins was achieved as previously described for rat RALDH2.[24,25] However, as stated above, differences in the chicken RALDH sequences necessitated the following modifications. RALDH1, 2, and 3/pET15b plasmids were transformed into BL21 (DE3) *Escherichiacoli* (New England Biolabs), according to the manufacturer's protocol and plated on LB agarose plates with carbenicillin selectivity (100 μg/mL; Sigma-Aldrich Corp.). Plates were placed in a 37°C incubator overnight. Bacterial colonies were gently removed from the plates and added to polypropylene round-bottomed tubes containing 5 mL LB and 100 μg/mL carbenicillin. Cultures were placed in a 37°C incubator shaker at 16*g* overnight. Then, 500 μL of the small cultures were added to 1 L flasks containing 250 mL LB broth and 100 μg/mL carbenicillin. Flasks then were placed in a 37°C incubator shaker at 16*g*, and the OD_{600} was checked hourly with a DU 800 spectrophotometer (Beckman Coulter) until the bacteria reached an OD_{600} of approximately 0.6 to 0.8. The temperature in the incubator shaker then was reduced to 16°C, and the bacteria were induced with 500 μM isopropyl-d-thiogalactopyranoside (IPTG; Sigma-Aldrich Corp.) for 24 hours. After 24 hours, bacteria were pelleted by centrifugation at 6,000*g* for 15 minutes at 4°C. Pellets were stored at −20°C until time of use.

To prepare purified protein from bacterial lysates, lysis buffer (50 mM Na_2HPO_4, 0.3 M NaCl, 5 mM imidazole, pH 8.0) containing 2 mM phenylmethylsulfonyl fluoride (PMSF; stock solution of 100 mM in isopropanol), 20 μg leupeptin (0.67 μg/mL), and 20 μg pepstatin (0.67 μg/mL) was added to the thawed pellets (30 mL per 1 L pellet). Pellets were resuspended in the buffer by vortexing vigorously. Cells were lysed using an Emulsiflex cell disruptor (Avestin, Inc.). Lysate was run through the disruptor twice and followed by a small volume of lysis buffer to ensure complete disruption and collection of lysates. After disruption, approximately 30 mg of deoxyribonuclease I (from bovine pancreas; Sigma-Aldrich Corp.) was added to the lysates and shook gently at RT for 45 minutes. Lysates then were centrifuged at 22,000*g* for 30 minutes at 4°C to pellet cellular debris, and the supernatant was collected.

Cobalt agarose beads used for purification were prepared by stripping nickel agarose beads and recharging with cobalt, as described below. Nickel agarose beads (Invitrogen) were loaded onto Poly-Prep chromotography columns (Bio-Rad) and 10 column volumes (CV) of 50 mM EDTA were loaded onto the column and allowed to flow through using a peristaltic pump (Pharmacia P-I Pump; GE Healthcare, Little Chalfont, United Kingdom) at a flow rate of 1.7 mL/minutes. Following EDTA stripping, 10 CVs of each of the following solutions were passed through the column: (1) 0.5 M NaOH, (2) dH_2O, (3) lysis buffer, (4) cobalt (II) chloride hexahydrate (5 mg/mL in dH_2O; Sigma-Aldrich), (5) lysis buffer.

Approximately 15 mL supernatant was loaded onto Poly-Prep chromotography columns (Bio-Rad) containing 2 mL cobalt agarose beads equilibrated in lysis buffer and allowed to flow through the column using a peristaltic pump (Pharmacia P-I Pump; GE Healthcare) at a flow rate of 1.7 mL/minutes. The column was washed with 5 CVs of lysis buffer, followed by 5 CVs of wash buffer (50 mM Na_2HPO_4, 0.3 M NaCl, 20 mM imidazole, pH 8.0). The RALDH proteins were eluted using a step gradient (50 mM Na_2HPO_4, 0.3 M NaCl, 50–1000 mM imidazole, pH 8.0; imidazole steps: 50, 100, 250, 500, 1000 mM). Elution of RALDH proteins was determined by SDS-PAGE using a 10% Bis-Tris Gel NuPAGE SDS-PAGE gel (Life Technologies, Grand Island, NY, USA) and standard protocols for the NuPAGE gel system, as described below. Gels were stained with SimplyBlue Safe Stain (Invitrogen) according to the manufactur-

Table 2. Immunogenic Peptides*

Protein	Peptide
RALDH2	ASLHLLPSPTLNLE-Cys
RALDH3	AAVNGAVENGPPDKKGPP-Cys

* Terminal cysteine (Cys) added to peptides to allow peptide conjugation to carrier protein.

er's instructions. Fractions containing the purified RALDH proteins were pooled and dialyzed against PBS.

Antibody Production

Polyclonal antibodies specific for chick RALDH2 and RALDH3 were generated in rabbits (Cocalico Biologicals, Inc., Reamstown, PA, USA). Peptides unique to each RALDH protein were synthesized (Table 2) and conjugated to keyhole limpet hemocyanin (KLH) protein. Intial inoculation and boosts were done according to the Cocalico's standard protocol (available in the public domain; http://www.cocalicobiologicals.com/antibodies.html). Antibodies were tested for specificity and relative titer during the course of production by Western blot analyses using purified, recombinant RALDH2 and 3. After significant immune responses were developed, rabbits were exsanguinated, and the whole serum was collected.

SDS-PAGE and Western Blot

To determine RALDH2 protein expression in chick ocular tissues, 10 μL of tissue homogenate or cytosol was prepared for SDS-PAGE and Western blot analysis, as described below. NuPAGE LDS Sample Buffer and NuPAGE Sample Reducing Agent were added to 10 μL of each sample so that the sample buffer and reducing agent came to a final concentration of 1× (Life Technologies). Samples then were placed in a 70°C water bath for 10 minutes and electrophoresed under reducing conditions on 10% Bis-Tris Gel NuPAGE SDS-PAGE gels (Life Technologies), according to standard protocols for the NuPAGE gel system. For Western blots, gels were electroblotted onto a nitrocellulose membrane (BioRad) using an electrotransfer unit (XCELL Sureback Electrophoresis Cell; Invitrogen) according to manufacturer's instructions. Blots were incubated in blocking buffer (0.2% I-Block; Tropix, Bedford, MA, USA and 0.1% Tween-20 in PBS) overnight at 4°C with gentle rocking. Blots then were incubated with rabbit anti-chick RALDH2 (1:500 in blocking buffer), rabbit anti-chick RALDH3 (1:500 in blocking buffer), or mouse anti-α-smooth muscle actin (1:500 in blocking buffer; Sigma-Aldrich) overnight at 4°C. Immunoblots were washed three times with PBS containing 0.05% Tween-20 followed by three washes with PBS. Immunoblots then were incubated with goat anti-rabbit IgG conjugated to alkaline phosphatase as a secondary labeling antibody (1:1,000 in PBS; BioRad). After incubation with the secondary antibody, blots were washed (as above), incubated in CDP-Star Ready-to-Use with Nitro-BlockII (Tropix) for 5 minutes, and images were captured with a Chemigenius imager (Syngene, Frederick, MD, USA).

Quantification of band intensity was performed using the Manual Band Quantification feature of the Syngene GeneTools (Syngene) program. The faintest band on each image was assigned a value of 1 and all other bands were automatically assigned relative values to the faintest band. Automatic background correction was applied.

Retinoic Acid Synthesis Assay

Retinaldehyde dehydrogenase activity was determined by measuring the production of atRA in vitro as described previously with minor modifications.[26] All procedures with all-trans-retinaldehyde or atRA were performed in dim red light. In duplicate, 200 μL of synthesis buffer (2.5% DMSO, 4 mM NAD, 32 mM tetrasodium pyrophosphate pH 8.2, 0.1 mM pyrazole, 5 mM glutathione, 1 mM EDTA) was added to 200 μL of cytosol from homogenized ocular tissues (in homogenization buffer). The reaction was initiated by the addition of 50 μL of 250 μM all-trans-retinaldehyde to the reaction mixture (25 μM final concentration). Negative controls included: (1) 200 μL of RALDH homogenization buffer in place of cytosol, (2) homogenization buffer in place of all-trans-retinaldehyde, and (3) absence of NAD. The reactions were mixed and placed in a water bath at 37°C for 0 to 60 minutes, after which time, the reactions were stopped by immersion in ice water and addition of 3/2 volumes (675 μL) of methanol. The samples were processed by HPLC, as described previously.[27]

Immunohistochemistry

An 8-mm punch was taken from the posterior ocular wall of control and recovering eyes, as descirbed above (see Tissue Isolation and Preparation). The retina and majority of RPE was removed, and choroids with sclera still attached, were placed into a 48-well flat bottom plate (Corning, Inc., Corning, NY, USA). A small amount of RPE was left on the choroids to discriminate between the RPE and scleral side of the tissue. Additionally, the scleral side of the choroid can be identified during imaging by the presence of large blood vessels and lymphatic lacunae located in the choroidal stroma. The tissues then were fixed with 4% paraformaldehyde (stock solution freshly prepared) in PBS overnight at 4°C. After fixation, choroids were gently removed from the scleral tissue, as described above, and placed into a new 48-well flat bottom plate (Corning Inc.). Choroids were washed in PBS for 10 minutes (6×) on a shaking device at RT. Choroids then were blocked in BSA-PBS (2% BSA, 0.2% Triton X-100, 0.004% sodium azide in PBS, pH 7.4) for 1 hour at RT with rocking and subsequently incubated in BSA-PBS containing rabbit anti-chick RALDH2 (1:50) for 5 days at 4°C. Choroids then were washed in PBS for 10 minutes (6×) at RT with rocking, incubated with goat anti-rabbit IgG conjugated to AlexaFluor 488 (1:1000 in PBS; Life Technologies) for 1 day at 4°C, and washed with PBS for 10 minutes (6×). Following the washes, choroids were coverslipped using a fluorescence mounting media (20 mM Tris, pH 8.0; 0.5% N-propyl gallate [Sigma-Aldrich]; 90% glycerol). Slides were stored at 4°C until imaging.

Choroids were viewed using a Fluoview 1000MPE multiphoton microscope (Olympus America, Inc., Center Valley, PA, USA), and z-stack images were collected through the entire thickness of the choroid (30–300 μm) with each slice representing 3 μm. Wallman et al.[28] have shown that the chick choroid expands considerably in response to myopic defocus to increase the speed of the recovery process ("choroidal accommodation"). Thus, the variation we observe in choroidal thickness is expected. Two 512 × 512 pixel areas (corresponding to 510 × 510 μm) were imaged for each of two choroids from control and recovering eyes at each time point. RALDH2-positive cells were counted manually in two representative regions of each pixel area in each slice to determine the number and distribution of positive cells per choroid.

Statistics

Analyses between groups were made using a 1-way ANOVA followed by a Bonferroni correction for multiple comparisons; analyses between pairs within a group were made using a paired or unpaired *t*-test (GraphPad Prism 5, La Jolla, CA, USA).

Investigative Ophthalmology & Visual Science

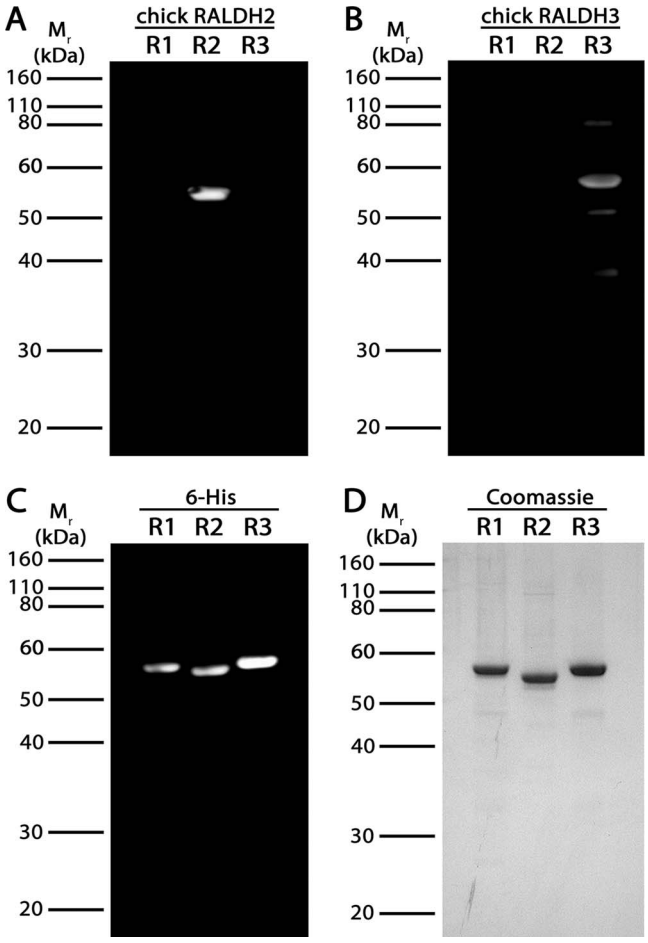

Figure 1. Western blot and SDS-PAGE analysis of recombinant chick RALDH1, 2, and 3. (**A**–**C**) Recombinant RALDH1, 2, and 3 (500 ng) were immunoblotted with anti-chick RALDH2 (**A**), anti-chick RALDH3 (**B**), or anti-6His (**C**). (**D**) 500 ng of purified, recombinant RALDH1 (R1), RALDH2 (R2), and RALDH3 (R3) were run on a 1.0 mm 10% Bis/Tris gel. RALDH1, 2, and 3 (~55–57 kDa) were greater than 90% pure, as determined by Coomassie Blue staining.

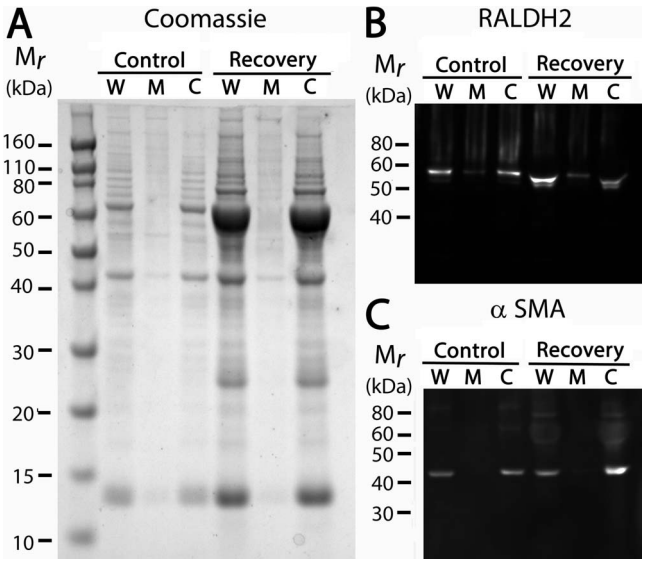

Figure 2. SDS-PAGE gel and Western blot analysis of choroidal RALDH2 and α-smooth muscle actin (αSMA) in various cellular fractions. (**A**) Whole tissue homogenates (W), microsomal fractions (M), and cytosol fractions (C) of control and 4-day recovering choroids were run on a 1.0 mm 10% Bis/Tris gel. (**B**, **C**) Identical gels were immunoblotted with anti-chick RALDH2 or anti-αSMA. RALDH2 immunopositive bands (~55–57 kDa) were detected strongly in the whole tissue homogenates and cytosol fractions of chick choroidal tissue, with faint detection in the microsomal fractions, while α-smooth muscle actin was detected solely in the whole tissue homogenates and cytosol fractions. A 10 μL amount of each sample was loaded per gel.

Results

RALDH Protein Expression in Chick Ocular Tissues

Antibodies specific for chick RALDH2 and RALDH3 were developed and tested on recombinant chick RALDH1 (R1), RALDH2 (R2), and RALDH3 (R3). Anti-RALDH1 antibodies were not developed as we have shown previously that RALDH1 mRNA cannot be detected in chick choroids.[17] Western blots of RALDH1, 2, and 3 probed with anti-chick RALDH2 and anti-chick RALDH3 confirmed antibody specificity to RALDH2 and RALDH3, respectively (Figs. 1A, 1B). Chick anti-RALDH2 detected a single band at approximately 55 kDa in only the lane containing RALDH2, while chick anti-RALDH3 detected a single band at approximately 57 kDa in only the lane containing RALDH3. Western blotting of RALDH1, 2, and 3 with an anti-6x-His antibody confirmed the proteins being detected were recombinantly expressed RALDH1, RALDH2, and RALDH3 containing the N-terminal 6-Histidine tag (Fig. 1C). All recombinant RALDH isoforms were greater than 90% pure as indicated by SDS-PAGE (Fig. 1D).

To further characterize the RALDH2 enzyme in chick choroids, Western blots were performed on subcellular fractions of control and day 4 recovering choroidal tissue to determine in which fraction RALDH2 was located (Fig. 2). Punches of 8 mm were taken from posterior eye cups, and choroids were isolated, as described above. Following a brief centrifugation of tissue homogenates at 12,000*g* for 20 sec to pellet cellular debris, whole tissue homogenate was spun at 100,000*g* to separate the microsomal fraction (pellet) from the soluble cytosol fraction. An SDS-PAGE gel of all fractions in control and recovering choroids indicated that recovering choroids contain approximately 6 to 8 times more protein compared to controls (508.3 ± 244.5 vs. 89.57 ± 35.31 ng/μL; Fig. 2A), which is due to increased vascular permeability and extravasation of serum proteins into the choroidal stroma of recovering samples.[29] Presence of the RALDH enzymes in the whole tissue homogenates (W), microsomal fractions (M), and cytosol fractions (C) then was determined by Western blot with the newly developed anti-chick RALDH2 antibody (Fig. 2B). Following Western blotting and detection, the approximately 55 kDa RALDH2 enzymes could be strongly detected in whole tissue homogenates and cytosol fractions, with negligible amounts detected in the microsomal fraction. An identical gel also was probed with anti-α-smooth muscle actin (αSMA), which served as a marker for cytosolic proteins (Fig. 2C). Based on the above results, the cytosolic fraction of tissue lysates was used in all subsequent experiments. In addition, Western blot analyses using anti-α-smooth muscle actin on choroid homogenates from control and recovering eyes indicated that the concentration of αSMA and, hence, choroid tissue volume, was very similar in 8 mm punches from control and recovering samples, indicating that normalizing to punch size is appropriate for our experiments.

Using the chick specific anti-RALDH2 and anti-RALDH3 antibodies, Western blot analysis was performed on cytosol fractions of retina/RPE, choroid, and sclera to determine the presence of these isoforms in chick ocular tissues ($n = 3$; Fig. 3). RALDH2 was detected strongly in the choroid (C) as a single

Investigative Ophthalmology & Visual Science

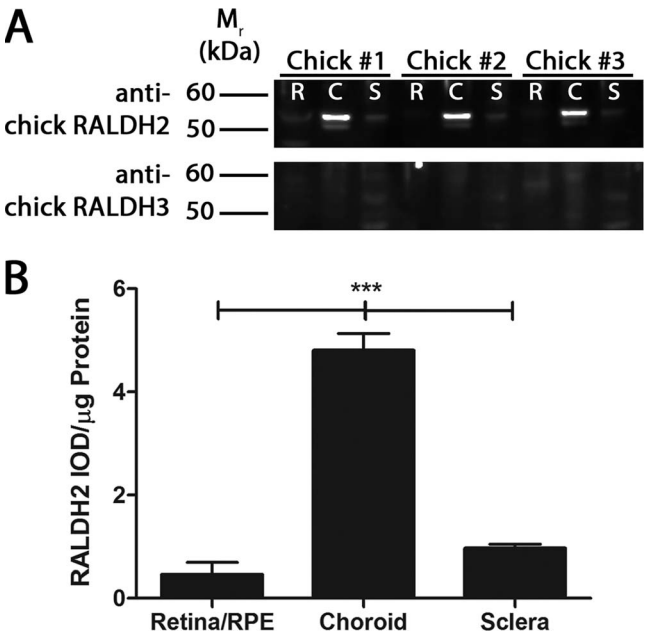

Figure 3. Western blot analysis and quantification of RALDH2 and RALDH3 in chick ocular tissues. (**A**) Cytosol fractions from chick ocular tissues were immunoblotted with anti-chick RALDH2 or anti-chick RALDH3. *Top*: RALDH2 immunopositive bands (~55 kDa) were present in choroid (C) of chick eyes and barely detectible in the retina/RPE (R) and sclera (S). *Bottom*: RALDH3 was not detected in any of the ocular tissues. Three μg total protein/lane was loaded for each blot. (**B**) Average abundance of RALDH2 (± SEM) in chick ocular tissues was measured as the integrated optical density (IOD) per μg protein of RALDH2-immunopositive bands ($n = 3$). ***$P < 0.001$ (1-way ANOVA followed by Bonferroni's multiple comparison test).

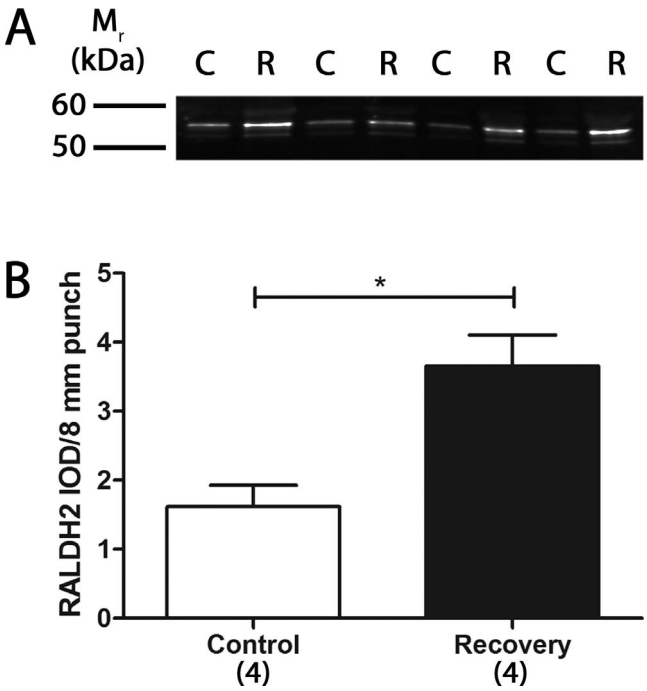

Figure 4. Western blot analysis and quantification of RALDH2 in control and 4-day recovering choroids. (**A**) Cytosol fractions from control (C) and day 4 recovering (R) choroids were immunoblotted with anti-chick RALDH2. RALDH2 immunopositive bands (~55 kDa) were present in control and recovering choroids. (**B**) Average RALDH2 abundance (± SEM) in control and day 4 recovering choroids was measured as the IOD per 8-mm biopsy punch ($n = 4$). *$P < 0.05$ (paired *t*-test).

band at approximately 55 kDa. RALDH2 was barely detectible in the retina/RPE (R) and sclera (S; Fig. 3A, top). RALDH3 was not detected in any of the ocular tissues (Fig. 3A, bottom). Quantification of the RALDH2 bands demonstrated that relative abundance of RALDH2 protein expression was highest in the choroid (4.81 ± 0.33 RALDH2 Integrated Optical Density [IOD]/μg protein], with low abundance in the sclera (0.97 ± 0.07 RALDH2 IOD/μg protein) and retina/RPE (0.47 ± 0.22 RALDH2 IOD/μg protein). Significant differences between the choroid and retina/RPE ($P < 0.001$, 1-way ANOVA with Bonferroni's multiple comparison test) and choroid and sclera ($P < 0.001$, 1-way ANOVA with Bonferroni's multiple comparison test) were observed. These results indicate that RALDH2 is expressed predominately in the chick choroid, with negligible amounts in the retina/RPE and sclera (Fig. 3B).

RALDH2 Protein Expression During Recovery From Induced Myopia

Previous studies have shown that the steady state mRNA levels of RALDH2 are significantly increased during recovery from induced myopia.[17] In the present study, RALDH2 protein expression was compared in 4-day control (C) and recovering (R) eyes by Western blot with chick specific anti-RALDH2 antibodies (Fig. 4A). The 4-day time point was used since RALDH2 mRNA levels were shown previously to be significantly increased at this time point.[17] Quantification of the band intensities demonstrated that RALDH2 protein levels were significantly increased in 4-day recovering choroids (3.65 ± 0.45 RALDH2 IOD/8-mm punch) compared to controls (1.62 ± 0.31 RALDH2 IOD/8-mm punch; $P < 0.05$, paired *t*-test; $n = 4$) (Figs. 4A, 4B). RALDH2 protein expression in 8-mm posterior choroidal punches was examined subsequently at several time points throughout the recovery process (0 hours to 15 days; Fig. 5). RALDH2 was detected in control and recovering choroids at all time points examined as an approximately 55 kDa band (Fig. 5A). Additionally, an immunopositive, closely spaced doublet migrating at 53 to 55 kDa was observed and became more apparent in control and recovering choroidal lysates from older chicks (following 10 days of form deprivation and 1–15 days of recovery). We suspect that this lower molecular weight band represents a partially degraded or alternatively spliced product of chick RALDH2, as we do not see this variant when chick RALDH2 is overexpressed in mammalian cell lines (data not shown) or in choroidal lysates of younger chick eyes. Quantification of the immunopositive bands indicated that RALDH2 protein expression was significantly increased in recovering choroids 24 hours (73.61 ± 15.04%; $P < 0.05$, Wilcoxon matched-pairs signed rank test) and 4 days (165.2 ± 65.9%; $P < 0.05$, Wilcoxon matched-pairs signed rank test) of recovery compared to control choroids ($n = 3$; Fig. 5B). No statistically significant differences were detected in RALDH2 protein expression between control and recovering choroids following 7 and 15 days of recovery ($P > 0.05$). In addition, during the course of recovery an age-dependent increase in RALDH2 protein expression in the contralateral, control eyes also was observed. To determine if this increase was due to a yoking effect between the control and experimental eyes or was the result of normal choroidal growth during the 28-day treatment period, an independent experiment using normal, untreated chicks (did not undergo form deprivation) was performed. As this study was performed on normal eyes, assessment of total choroidal protein was not complicated by changes in vascular permeability and extravasation of serum protein into the choroidal stroma that we

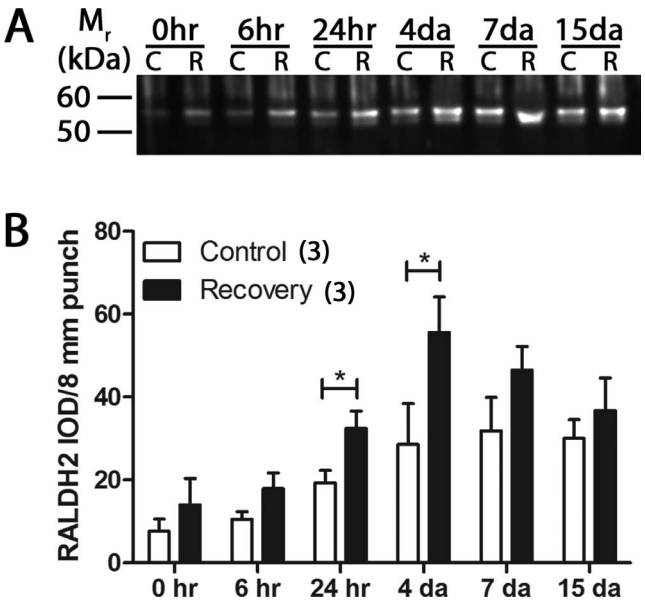

FIGURE 5. Western blot analysis and quantification of RALDH2 in choroids over a 15-day recovery period. (**A**) Cytosol fractions from control (C) and recovering (R) choroids were immunoblotted with anti-chick RALDH2 at various time points during the course of recovery. RALDH2 immunopositive bands (~55 kDa) were present in control and recovering choroids at all time points examined. Blot shown is representative of 3 independent blots. (**B**) Average RALDH2 abundance (± SEM) in control and recovering choroids was measured as the IOD per 8 mm biopsy punch ($n = 3$ for each time point). $^{*}P < 0.05$ (Wilcoxon matched-pairs signed rank test).

observe during recovery. Thus, results were normalized to total protein in this particular experiment. RALDH2 protein was observed to increase significantly in normal choroids over a 15-day time period; however, after normalization to total choroidal protein (increased from 150 ± 46.7 ng/μL in choroids from 10-day-old chicks to 431.7 ± 61.6 ng/μL in choroids from 28-day-old chicks), no change in RALDH2 protein expression was observed in these choroids (data not shown).

RALDH Activity During Recovery From Induced Myopia

To determine if the increase observed in RALDH2 protein expression in recovering choroids results in an increase in atRA synthesis, RALDH activity was examined in the ocular tissue cytosol fractions using an atRA synthesis assay (Fig. 6). To examine the kinetics of the assay, cytosol fractions from untreated choroids were incubated at 37°C with all-trans-retinaldehyde (25 μM) for 0 to 60 minutes, and atRA was measured at various points (Fig. 6A). atRA synthesis was linear from 0 to 60 minutes of incubation; thus, all subsequent assays were conducted for 30 minutes. Since the stoichiometry of the reaction is 1:1, the amount of all-trans-retinaldehyde converted to atRA during the reaction (20–200 pmoles) is at least 5 orders of magnitude less than the concentration of all-trans-retinaldehyde present in the reaction (25 μM), ensuring that the substrate concentration is not rate-limiting. RALDH activity was measured in retina/RPE, choroid, and sclera of control and day 4 recovering eyes and was only detectible in the choroids ($n = 9$; Fig. 6B). RALDH activity was significantly higher in recovering choroids (138.80 ± 13.03 pmol/h/8-mm punch) compared to controls (58.62 ± 6.94 pmol/h/8-mm punch) ($P < 0.001$, paired t-test). RALDH activity also was examined in choroidal cytosol fractions of control and recovering eyes at

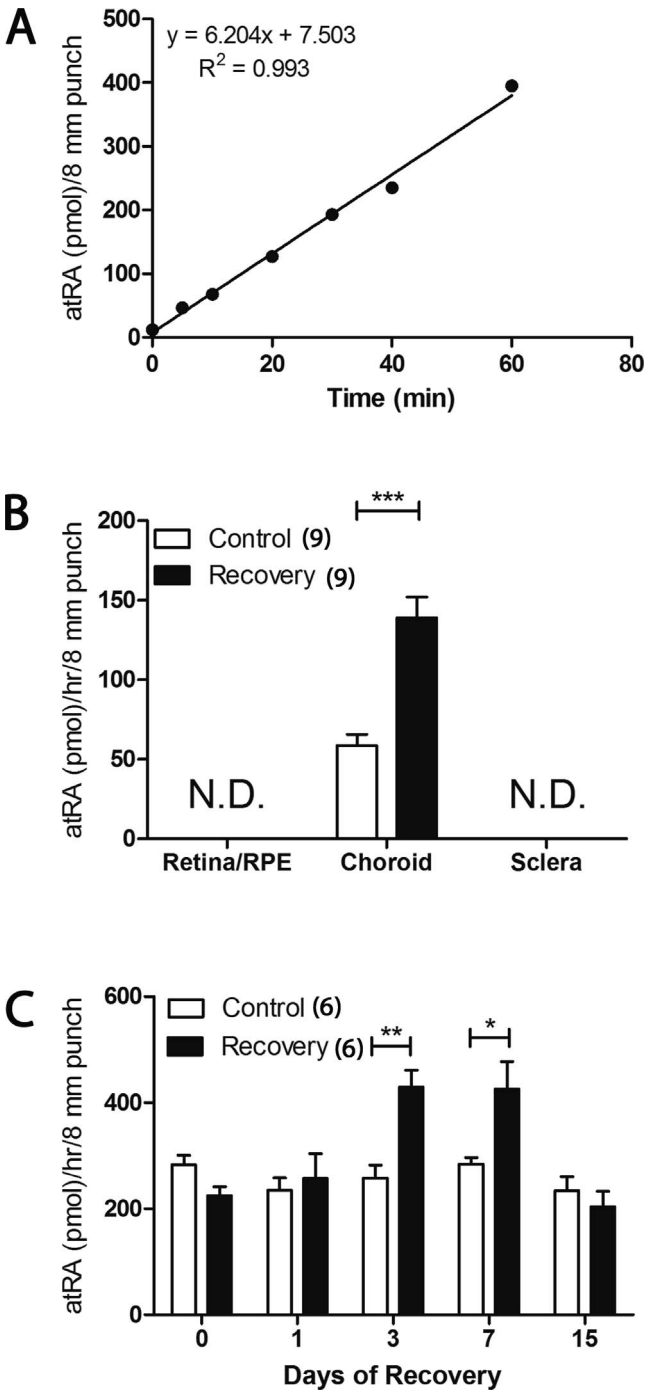

FIGURE 6. RALDH enzymatic activity in control and recovering chick ocular tissues using a HPLC/spectrophotometric assay for NAD-dependent atRA synthesis. (**A**) atRA synthesis is linear in untreated choroidal lysates from 0 to 60 minutes. All subsequent synthesis assays were conducted for 30 minutes. (**B**) Average RALDH enzymatic activity (± SEM) in chick ocular tissues in control and day 4 recovering eyes ($n = 9$). Activity was not detectible (N.D.) in the retina/RPE or sclera. (**C**) Average RALDH enzymatic activity (± SEM) in control and recovering choroids at various time points during the course of recovery ($n = 6$ measurements for each time point). Each activity measurement represents the average of two duplicate samples. $^{*}P < 0.05$, $^{**}P < 0.01$, $^{***}P < 0.001$ (paired t-test).

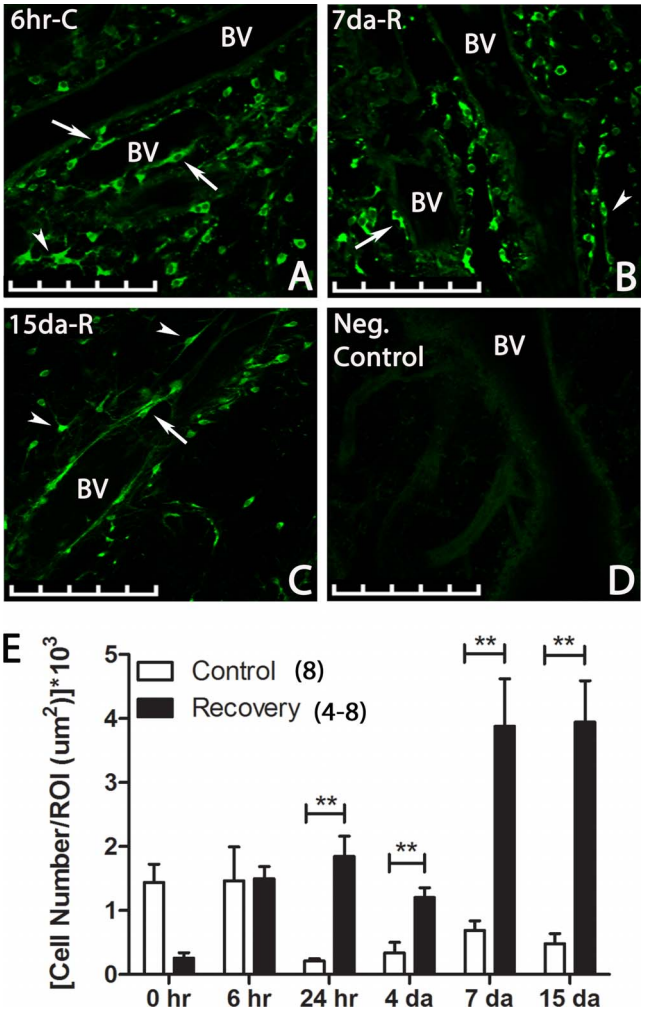

Figure 7. Multiphoton images and quantification of RALDH2 expressing cells (*green*) in control and recovering choroids after immunolabeling with the anti-chick RALDH2 antibody. (**A–C**) Images of representative RALDH2 immunopositive cells in choroids throughout recovery. RALDH2 labeling was detected in round or spindle-shaped cell bodies with some cells exhibiting long, thin projections (*arrowhead*). Some choroidal stromal cells were located in close association with blood vessels (*arrow*). BV, blood vessel; 6hr-C, 6-hour control; 7da-R, 7-day recovery; 15da-R; 15-day recovery. (**D**) Negative control choroid (incubation in preimmune rabbit serum instead of primary antibody) demonstrating absence of labeling in the tissue. *Scale bars*: 100 μm in (**A–D**). (**E**) Average total RALDH2 cell number (± SEM) in control and recovering choroids (30–300 μm thick z-stacks) at various time points throughout recovery. Results were normalized to cross-sectional area for each ROI selected to perform the counting (n = 4–8). $^{**}P < 0.01$ (paired t-test).

different time points during recovery (Fig. 6C). Synthesis of atRA was similar in control and recovering choroids at 0 hours and 1 day of recovery ($P > 0.05$). Synthesis significantly increased in recovering choroids at 3 (70.13 ± 13.25%; $P < 0.01$, paired t-test) and 7 days (48.47 ± 14.75%; $P < 0.05$, paired t-test) of recovery with atRA levels returning to control levels by 15 days of recovery ($n = 6$).

Distribution of RALDH2 Cells in Chick Choroidal Tissue

The distribution of RALDH2 immunopositive cells in the chick choroid was evaluated by multiphoton microscopy (Fig. 7). RALDH2 immunopositive cells (green) were present at all time points examined and were characterized by round or spindle-shaped cell bodies with some exhibiting long, thin projections/processes (Figs. 7A–C, arrowhead). RALDH2 immunopositive cells have an average cell size of 62.94 ± 2.89 μm^2, with an average nuclear size of 28.40 ± 1.17 μm^2. A subpopulation of RALDH2 immunopositive cells contained 1 to 2 processes, extending from opposite poles of the cell body, with the average length of the processes measuring 20.45 ± 1.98 μm. No labeling was seen when choroids were incubated in preimmune rabbit serum in place of primary antibody (Fig. 7D). RALDH2 immunolabeling was detected in cells throughout the choroidal stroma with some extravascular stromal cells in close association with blood vessels (Figs. 7A–C, arrow). Following 10 days of form deprivation (0 hours recovery), the total number of RALDH2 immunopositive cells present throughout the entire thickness of choroids was higher in control eyes (1.44 ± 0.28 RALDH2-positive cells/cross-sectional region of interest [ROI]) compared to recovering eyes (0.26 ± 0.08 RALDH2-positive cells/ROI) at 0 hours of recovery, although this increase was not statistically significant (P = 0.0538; n = 4–8; Fig. 7E). The number of RALDH2-positive cells was similar between control and recovering choroids following 6 hours of recovery but increased significantly in recovering choroids at 24 hours (1.84 ± 0.31 RALDH2-positive cells/ROI in recovering eyes compared to 0.21 ± 0.04 RALDH2-positive cells/ROI in controls; $P < 0.01$, paired t-test), 4 days (1.20 ± 0.15 RALDH2-positive cells/ROI in recovering eyes compared to 0.33 ± 0.17 RALDH2-positive cells/ROI in controls; $P < 0.01$, paired t-test), 7 days (3.87 ± 0.74 RALDH2-positive cells/ROI in recovering eyes compared to 0.69 ± 0.15 RALDH2-positive cells/ROI in controls; $P < 0.01$, paired t-test), and 15 days (3.95 ± 0.64 RALDH2-positive cells/ROI in recovering eyes compared to 0.48 ± 0.16 RALDH2-positive cells/ROI in controls; $P < 0.01$, paired t-test) compared to control choroids.

To determine the distribution of RALDH2 immunopositive cells throughout the thickness of the choroid, the percentage of RALDH2 cells located in each 3 μm^2 slice was compared from Bruch's membrane (0 μm) to the scleral side of the choroid (Fig. 8). Note that data in Figure 8 represent the percentage of total RALDH2-positive cells located in each slice regardless of their absolute number. As indicated in Figure 7E, there are significant differences in the number of RALDH2 cells in the chick choroids of control and recovering eyes. In control choroids at all time points examined, RALDH2-positive cells were distributed relatively evenly throughout the choroid. Similarly, RALDH2 cells in recovering choroids at 6 and 24 hours were distributed throughout the thickness of the choroid (Figs. 8B, 8C). Interestingly, RALDH2 cells in form-deprived choroids immediately before recovery (0 hours) were located on the scleral and RPE sides of the choroid with relatively few in the center (Figs. 8D–G). In contrast, following 4 to 15 days of recovery, RALDH2-positive cells were concentrated toward the RPE side of the choroid, with relatively few cells on the scleral side.

Discussion

Retinoic acid has been implicated in the signaling cascade that modulates eye growth between the retina and the sclera.[11,16,29] The chick choroid has been shown to synthesize relatively high levels of atRA, compared to the retina or liver, and the rate of atRA synthesis is dramatically affected by the refractive state of the eye. Choroidal synthesis of atRA is increased in chick eyes during recovery from induced myopia and during compensation for imposed myopic defocus (using plus lenses), and atRA was shown to be decreased in eyes undergoing form

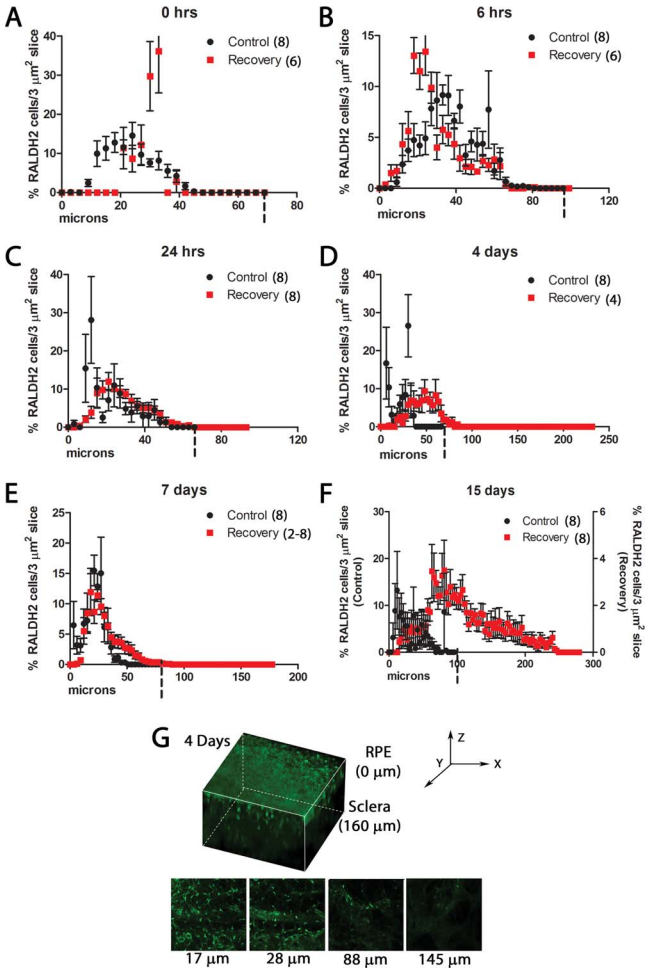

Figure 8. Distribution of RALDH2 immunopositive cells throughout the thickness of control and recovering choroids. (**A–F**) Percentage of RALDH2 cells located in each 3 μm² slice of z-stack images obtained in Figure 7 in control (*black*) and recovering (*red*) choroids at various time points throughout recovery ($n = 2$–8 regions per cross sectional area). The side of the choroid closest to Bruch's membrane was designated at 0 μm. *Dashed vertical bars* on *x*-axis represent total thickness of control choroids (which were substantially thinner than recovering choroids following 24 hours of recovery). *(**F**) Data from 15-day recovering choroids is plotted on an expanded *y*-axis to demonstrate relative RALDH2 distribution across choroid. (**G**) 3D reconstruction of a z-stack obtained by multiphoton from a 4-day recovering choroid. RALDH2 immunopositive cells (*green*) are found closer to the RPE side of the choroid (0 μm) than to the scleral side of the choroid (160 μm). Single images represent single slices taken throughout the thickness of the choroid. Micrometers under all images indicate distance from the scleral side of the choroid.

deprivation myopia and compensation for hyperopic defocus (using minus lenses). Interestingly, the time course of the increase in choroidal atRA synthesis[16] was remarkably similar to that of the decrease in rate of scleral proteoglycan synthesis observed in the early phase of recovery from induced myopia,[29] suggesting a causal relationship between choroidal atRA synthesis and scleral proteoglycan synthesis.[30] Moreover, the endogenous concentrations of atRA generated by choroids in vitro were within the range to produce significant inhibition of scleral proteoglycan synthesis.[17] Taken together, these studies suggested that choroidal synthesis of atRA in response to visual stimuli may modulate scleral proteoglycan synthesis.

Changes in choroidal atRA synthesis in response to visual stimuli also have been described in mammals. In guinea pigs and primates, atRA synthesis is increased in the choroid/sclera[20] and RPE/choroid,[18] respectively, during the development of myopia, a condition that is associated with decreased scleral proteoglycan synthesis. However, in contrast to chicks, decreased proteoglycan synthesis in the mammalian sclera is associated with increased axial elongation.[5,8,31] Similar to chicks, atRA has been demonstrated to inhibit proteoglycan synthesis in the primate sclera.[18] Therefore, in chicks and primates, the visually-induced changes in choroidal atRA synthesis and concentration are consistent with the known changes in scleral proteoglycan synthesis that occur during visually-guided ocular growth and may represent an evolutionarily conserved mechanism for visually-guided ocular growth regulation.

Previous work has suggested that choroidal atRA synthesis may be regulated by changes in the atRA synthesizing enzyme, RALDH2, as *RALDH2* transcript levels are elevated in the chick choroid during recovery from form deprivation–induced myopia, while no changes were identified in transcript levels of other retinoic acid synthesizing or catabolizing enzymes (*RDH 10*, *RALDH3*, *Cyp1B1*, *Cyp26*).[16,17] Therefore, the objective of the current investigation was to determine if changes in *RALDH2* transcript levels result in changes in RALDH2 protein expression and RALDH enzyme activity in chick ocular tissues during recovery from induced myopia.

RALDH Protein Expression During Recovery From Induced Myopia

Western blot analyses of chick ocular tissue lysates indicated that RALDH2 was the sole RALDH isoform present in chick ocular tissues and was predominately expressed in the choroid (Fig. 3). Protein expression of RALDH2 agrees with the data of Rada et al.[17] data, which found that *RALDH2* transcript was expressed in low amounts in the retina and in comparatively high amounts in the choroid. However, despite Rada et al.[17] observing very low levels of *RALDH3* transcript in the chick retina and choroid, we did not detect RALDH3 protein in any of the chick ocular tissues using the anti-chick RALDH3 antibody. It is possible that the levels of RALDH3 present in the chick ocular tissues are too low to detect or that the mRNA is not translated. Thus, our results suggested that RALDH2 is the only RALDH enzyme present in the choroid and, as such, is responsible for choroidal generation of atRA.

Interestingly, RALDH2 migrates as a closely-spaced doublet with a major immunopositive band present at approximately 55 kDa and a minor band present between 53 and 55 kDa. The presence of this minor band became more apparent in control and recovering choroidal lysates of older chicks. In postnatal human eyes, aged 16 to 46 years, RALDH2 also migrates as a doublet with a major immunopositive band migrating at approximately 55 kDa and a minor band migrating at approximately 59 kDa.[32] As human RALDH2 has four known splice variants, the doublet present in human ocular tissues is attributed to various splice variants of the RALDH2 protein. However, as there currently are no known splice variants for chicken RALDH2, we suspect that the lower molecular weight immunopositive band in chick choroids may be due to aging-associated degradation of RALDH2. As the postnatal expression of RALDH2 is limited to few tissues, including the testis, lung, and liver,[33–35] it is possible that similar processing of RALDH2 occurs in other chicken tissues and organs. Moreover, this processing does not seem to affect RALDH enzymatic activity, as the rate of retinoic acid synthesis was similar in choroids of all control eyes over the 15-day recovery period.

During recovery from induced myopia, RALDH2 protein expression is significantly increased at 24 hours and 4 days of recovery, with levels returning to control levels by 7 days.

Investigative Ophthalmology & Visual Science

These results closely followed the increase observed in *RALDH2* transcript levels,[17] thus providing further evidence for the idea that RALDH2 expression is modulated during recovery to effect change on scleral extracellular matrix remodeling. We also observed an increase in RALDH2 expression in control eyes over the course of recovery, though this increase was not as prominent as that observed over the 15-day recovery period. However, additional experiments on normal aged-match chicks indicated that increases in RALDH2 protein expression paralleled increases in total protein expression in normal choroids of birds aged 10 to 28 days old (data not shown). Therefore, we attribute increases in RALDH2 protein expression observed in control eyes over the 15-day treatment period to undergo an age-dependent increase as a consequence of normal choroidal tissue growth and maturation. It is interesting to consider that increases in RALDH2 protein expression in the choroids of normal birds may have a role in the normal slowing of eye elongation during aging, as atRA has a role in scleral extracellular matrix remodeling.[16–18] In recovering eyes, this growth-related increase in RALDH2 is most likely present, but further surpassed by additional recovery-induced increases in RALDH2 protein expression. Alternatively, age-related increases in RALDH2 protein expression may reflect sampling from RALDH2-enriched regions of the choroid that become more regionalized with age in larger eyes. As mentioned previously, normalizing recovering choroids to total protein is problematic, as recovery is associated with increased vascular permeability.[23] Interestingly, the increase in RALDH2 protein observed from 6 hours to 7 days in control eyes was not reflected in an increase of RALDH activity (Fig. 6), suggesting the presence of endogenous choroidal proteins that may act to modulate RALDH2 activity.

RALDH Activity During Recovery From Induced Myopia

It has been suggested that atRA, through its action on scleral proteoglycan synthesis, is responsible for changes in ocular growth rates and refraction.[16–18] Therefore, it is of great interest to identify the ocular tissues and cells responsible for atRA synthesis during postnatal ocular growth. Comparisons of RALDH activity in the retina/RPE, choroid, and sclera indicated that the choroid is the only ocular tissue in the chick that synthesizes atRA. No RALDH activity could be detected in the chick retina/RPE or sclera. Our findings agreed with those presented by Mertz and Wallman,[16] who found that the choroid is able to produce approximately 20 times more atRA compared to the retina, while no atRA could be detected in the sclera. As RALDH2 was the only RALDH isoform detected in the chick ocular tissues and was in highest concentration in the choroid compared to other ocular tissues, this suggested that the vast majority of the ocular synthesis of atRA is due to choroidal expression of RALDH2.

During the course of recovery, choroidal RALDH activity was significantly increased at 3 and 7 days of recovery and returned to control levels by 15 days. Interestingly, the increase in RALDH activity lagged somewhat behind the increase in RALDH2 protein expression, which began to increase at 24 hours of recovery, peaked at 4 days, and returned to control levels by 7 days of recovery. As our measurements of RALDH activity were performed on choroidal tissue lysates using an in vitro assay in the presence of excess all-trans-retinaldehyde, we suspect that other factors must be at work to suppress RALDH2 activity in vivo even in the presence of increased RALDH2 enzyme concentrations. For example, it is well established that, in vivo, the RDH enzymes may modulate atRA biosynthesis by regulating the availability of RALDH substrate, as they are known to be the rate limiting step in atRA biosynthesis.[21,36] However, in a previous publication, we did evaluate the expression of RDH 10 during recovery and found no changes in gene expression between control and recovering choroids over the 15-day recovery period.[17] Additionally, in vivo, retinoids are bound to high-affinity, high-specificity binding proteins that facilitate their metabolism and thereby modulate steady-state concentrations of atRA.[37] Specifically, the rate of atRA synthesis by RALDH2 is increased approximately 2-fold when retinaldehyde is complexed to cellular retinol binding protein (CRBP) compared to free retinaldehyde.[24] By inference, the absence of binding proteins in our in vitro RALDH2 activity assays may result in an underestimation of in vivo RALDH2 activity in control and recovering choroids. Further, the presence of potential cytosolic inhibitors (unknown at this time) would be present in our choroidal cytosol fractions and likely inhibit RALDH2 activity in vitro, even in the presence of increased RALDH2 protein levels.

Distribution of RALDH2 Cells in Chick Choroidal Tissue

Two previous studies suggest that atRA is produced at the posterior margin of the choroid in close proximity to the sclera, where it could be transported efficiently to target cells in the sclera with minimal diffusional loss.[16,38] Since results of the present study show that RALDH2 is the only atRA-synthesizing enzyme in the chick choroid, the distribution of RALDH2 expressing cells is likely to reflect the sites of atRA synthesis in the choroid. Therefore, to identify areas of atRA synthesis in the choroid, choroids were immunolabeled with anti-chick RALDH2, and the distribution of RALDH2 immunopositive cells was quantified in control and recovering eyes over a 15-day time period.

In the choroid, RALDH2 immunopositive cell bodies were round or spindle shaped, in agreement with previous findings.[17] We have shown previously that some of the RALDH2 expressing cells also express α-smooth muscle actin.[17] However, these cells do not express CD-45 (Harper AR, et al. *IOVS* 2015;56:ARVO E-abstract 5845) or neuron specific β-III tubulin (Jody Summers, personal communication, 2015), indicating that these cells are not of hematopoietic or neuronal origin, respectively. Currently, we speculate that the RALDH2-positive cells may be a subpopulation of smooth muscle cells or possibly a type of extrahepatic stellate cell,[39,40] as hepatic stellate cells are known to contain RALDH enzymes and to produce atRA.[41,42] Work currently is ongoing in our lab to further characterize this cell population, as it may represent a unique population of cells in the choroid.

The absolute number of RALDH2 immunopositive cells in a 510 × 510 μm region of choroid from the posterior pole increased significantly following 24 hours, and 4, 7, and 15 days of recovery compared to control eyes in the same region. These results agreed with the Western blot and RALDH activity data and also correlated very well with our previous findings measuring the absolute amount of atRA in recovering choroids.[17] However, some discrepancies do exist, particularly at the 7- and 15-day time points. In the Western blot and activity data, protein and activity levels eventually returned to control levels, while by immunostaining, these levels remained highly elevated at these later time points. Differences observed among the Western blot, immunostaining, and RALDH activity may be due to differences in the sensitivities of the techniques, as discussed above. Moreover, it has been shown that antibodies may exhibit different sensitivities between Western blot and immunostaining.[43,44] It is unlikely that antigen accessibility

Investigative Ophthalmology & Visual Science

or antibody penetration during choroid tissue immunolabeling was responsible for the observed differences, as relatively long incubation periods with anti-chick RALDH2 antibody (5 days) were used routinely. Further, in our immunohistochemistry experiments, cells were counted based on the presence or absence of RALDH2; the intensity of immunostaining was not assessed. Therefore, while the absolute number of cells expressing RALDH2 may be higher at 7 and 15 days of recovery compared to controls, the relative abundance of RALDH2 present in these cells may be lower than at earlier time points, more similar to controls. Interestingly, our results indicated that the number of RALDH2-positive cells was lower following 10 days of form deprivation (0 hours) in treated eyes compared to controls, although this decrease was not statistically significant ($P = 0.0538$). While we did not observe a decrease in RALDH2 protein expression by Western blot or a decrease in RALDH activity in form deprived eyes, Mertz and Wallman[16] demonstrated that choroidal [^{3}H]-atRA synthesis decreased in response to form deprivation, when using [^{3}H]-retinol as a substrate. Taken together, these results suggested that atRA synthesis may be bidirectionally regulated in the choroid either through RALDH2 protein expression and/or regulation of RALDH activity, as well as by the number and distribution of RALDH2 expressing cells in the choroid.

Interestingly, in addition to an increased number of RALDH2-positive cells, the distribution of RALDH2 immunopositive cells throughout the choroid shifted during the recovery from myopia. Following 4 to 15 days of recovery, a greater percentage of RALDH2 immunopositive cells were found closer to Bruch's membrane and the RPE than to the sclera. Mertz and Wallman[16] had previously suggested that atRA synthesis may be located closer to the sclera so that atRA could quickly mediate its effects on the sclera. In contrast, we showed that RALDH2 cells are located on the inner side of the choroid close to the RPE. In this position, the RALDH2 expressing cells would be poised to receive a signal(s) directly from the retina and/or RPE in response to myopic defocus. In response to this signal, we speculated that choroidal cells would then increase levels of RALDH2 which would, in turn, increase the production of atRA. We further speculated that atRA generation close to the RPE would necessitate the presence of transport proteins to carry atRA to the sclera to modulate scleral proteoglycan synthesis and initiate recovery. In addition, atRA also may be involved in lymphatic changes observed in the choroid during recovery given that the lymphatics lie in between the RPE and sclera, and seem to change dramatically during recovery.[45,46] Retinoic acid is required for the differentiation of precursor lymphatic endothelial cells (LEC) into mature LECs during murine development,[47] and 9 cis-RA promotes lymphangiogenesis and enhances lymphatic vessel regeneration in models of lymphedema.[48] Thus, it is possible that atRA also may have a role in the increase in lymphatic vessel volume observed during recovery.

In summary, the results of the present study demonstrated that choroidal RALDH2 protein expression and RALDH enzymatic activity are increased in the chick eye during recovery from form deprivation myopia. Furthermore, RALDH2 is expressed by a population of choroidal cells that become concentrated at the inner side of the choroid, adjacent to the RPE. Recently, RALDH1 and RALDH2 have been identified in the postnatal human eye as well, suggesting that RALDH2 and atRA may have a role in postnatal ocular growth of humans.[33] As such, RALDH2 may represent a potential therapeutic target to modulate postnatal ocular growth.

Acknowledgments

The authors thank John Moore, research assistant, from the Department of Cell Biology at the University of Oklahoma Health Sciences Center for technical assistance.

Supported by National Eye Institute Grant R01 EY09391 (JAS), EY012231 (JxM), and National Eye Institute Fellowship F31EY025168 (ARH).

Disclosure: **A.R. Harper**, None; **X. Wang**, None; **G. Moiseyev**, None; **J.-X. Ma**, None; **J.A. Summers**, None

References

1. O'Leary DJ, Millodot M. Eyelid closure causes myopia in humans. *Experientia*. 1979;35:1478–1479.
2. Rabin J, Van Sluyters RC, Malach R. Emmetropization: a vision-dependent phenomenon. *Invest Ophthalmol Vis Sci*. 1981;20:561–564.
3. Rasooly R, BenEzra D. Congenital and traumatic cataract. The effect on ocular axial length. *Arch Ophthalmol*. 1988;106:1066–1068.
4. Twomey JM, Gilvarry A, Restori M, Kirkness CM, Moore AT, Holden AL. Ocular enlargement following infantile corneal opacification. *Eye (Lond)*. 1990;4:497–503.
5. Norton TT, Rada JA. Reduced extracellular matrix in mammalian sclera with induced myopia. *Vision Res*. 1995;35:1271–1281.
6. Wallman J, Turkel J, Trachtman J. Extreme myopia produced by modest change in early visual experience. *Science*. 1978;201:1249–1251.
7. Howlett MH, McFadden SA. Form-deprivation myopia in the guinea pig (Cavia porcellus). *Vision Res*. 2006;46:267–283.
8. Rada JA, Nickla DL, Troilo D. Decreased proteoglycan synthesis associated with form deprivation myopia in mature primate eyes. *Invest Ophthalmol Vis Sci*. 2000;41:2050–2058.
9. Rada JA, Thoft RA, Hassell JR. Increased aggrecan (cartilage proteoglycan) production in the sclera of myopic chicks. *Dev Biol*. 1991;147:303–312.
10. Wallman J, Adams JI. Developmental aspects of experimental myopia in chicks: susceptibility, recovery and relation to emmetropization. *Vision Res*. 1987;27:1139–1163.
11. Summers JA. The choroid as a sclera growth regulator. *Exp Eye Res*. 2013;114:120–127.
12. Wallman J. Retinal influences on sclera underlie visual deprivation myopia. *Ciba Foundation Symposium*. 1990;155:126–134; discussion 135–141.
13. Pendrak K, Nguyen T, Lin T, Capehart C, Zhu X, Stone RA. Retinal dopamine in the recovery from experimental myopia. *Curr Eye Res*. 1997;16:152–157.
14. Stone RA, Lin T, Laties AM, Iuvone PM. Retinal dopamine and form-deprivation myopia. *Proc Natl Acad Sci U S A*. 1989;86:704–706.
15. Fischer AJ, McGuire JJ, Schaeffel F, Stell WK. Light- and focus-dependent expression of the transcription factor ZENK in the chick retina. *Nat Neurosci*. 1999;2:706–712.
16. Mertz JR, Wallman J. Choroidal retinoic acid synthesis: a possible mediator between refractive error and compensatory eye growth. *Exp Eye Res*. 2000;70:519–527.
17. Rada JA, Hollaway LY, Li N, Napoli J. Identification of RALDH2 as a visually regulated retinoic acid synthesizing enzyme in the chick choroid. *Invest Ophthalmol Vis Sci*. 2012;53:1649–1662.
18. Troilo D, Nickla DL, Mertz JR, Summers Rada JA. Change in the synthesis rates of ocular retinoic acid and scleral glycosaminoglycan during experimentally altered eye growth in marmosets. *Invest Ophthalmol Vis Sci*. 2006;47:1768–1777.

19. Seko Y, Shimizu M, Tokoro T. Retinoic acid increases in the retina of the chick with form deprivation myopia. *Ophthalmic Res*. 1998;30:361–367.
20. McFadden SA, Howlett MH, Mertz JR. Retinoic acid signals the direction of ocular elongation in the guinea pig eye. *Vision Res*. 2004;44:643–653.
21. Napoli JL. Effects of ethanol on physiological retinoic acid levels. *IUBMB Life*. 2011;63:701–706.
22. Simon P, Feldkaemper M, Bitzer M, Ohngemach S, Schaeffel F. Early transcriptional changes of retinal and choroidal TGFbeta-2, RALDH-2, and ZENK following imposed positive and negative defocus in chickens. *Mol Vis*. 2004;10:588–597.
23. Rada JA, Palmer L. Choroidal regulation of scleral glycosaminoglycan synthesis during recovery from induced myopia. *Invest Ophthalmol Vis Sci*. 2007;48:2957–2966.
24. Wang X, Penzes P, Napoli JL. Cloning of a cDNA encoding an aldehyde dehydrogenase and its expression in Escherichia coli. Recognition of retinal as substrate. *J Biol Chem*. 1996;271:16288–16293.
25. Lamb AL, Newcomer ME. The structure of retinal dehydrogenase type II at 2.7 A resolution: implications for retinal specificity. *Biochemistry*. 1999;38:6003–6011.
26. McCaffery P, Lee MO, Wagner MA, Sladek NE, Drager UC. Asymmetrical retinoic acid synthesis in the dorsoventral axis of the retina. *Development*. 1992;115:371–382.
27. Farjo KM, Moiseyev G, Nikolaeva O, Sandell LL, Trainor PA, Ma JX. RDH10 is the primary enzyme responsible for the first step of embryonic Vitamin A metabolism and retinoic acid synthesis. *Dev Biol*. 2011;357:347–355.
28. Wallman J, Wildsoet C, Xu A, et al. Moving the retina: choroidal modulation of refractive state. *Vision Res*. 1995;35:37–50.
29. Summers Rada JA, Hollaway LR. Regulation of the biphasic decline in scleral proteoglycan synthesis during the recovery from induced myopia. *Exp Eye Res*. 2011;92:394–400.
30. Harper AR, Summers JA. The dynamic sclera: extracellular matrix remodeling in normal ocular growth and myopia development. *Exp Eye Res*. 2015;133:100–111.
31. Rada JA, Achen VR, Penugonda S, et al. Proteoglycan composition in the human sclera during growth and aging. *Invest Ophthalmol Vis Sci*. 2000;41:1639–1648.
32. Harper AR, Wiechmann AF, Moiseyev G, Ma JX, Summers JA. Identification of active retinaldehyde dehydrogenase isoforms in the postnatal human eye. *PLoS One*. 2015;10:e0122008.
33. Wu JW, Wang RY, Guo QS, Xu C. Expression of the retinoic acid-metabolizing enzymes RALDH2 and CYP26b1 during mouse postnatal testis development. *Asian J Androl*. 2008;10:569–576.
34. Owusu SA, Ross AC. Retinoid homeostatic gene expression in liver, lung and kidney: ontogeny and response to vitamin A-retinoic acid (VARA) supplementation from birth to adult age. *PLoS One*. 2016;11:e0145924.
35. Ogura Y, Suruga K, Mochizuki H, Yamamoto T, Takase S, Goda T. Postnatal changes in gene expression of retinal dehydrogenase and retinoid receptors in liver of rats. *Life Sci*. 2004;74:1519–1528.
36. Napoli JL. Physiological insights into all-trans-retinoic acid biosynthesis. *Biochim Biophys Acta*. 2011;1821:152–167.
37. Napoli JL, Boerman MH, Chai X, Zhai Y, Fiorella PD. Enzymes and binding proteins affecting retinoic acid concentrations. *J Steroid Biochem Mol Biol*. 1995;53:497–502.
38. Fischer AJ, Wallman J, Mertz JR, Stell WK. Localization of retinoid binding proteins, retinoid receptors, and retinaldehyde dehydrogenase in the chick eye. *J Neurocytol*. 1999;28:597–609.
39. Nagy NE, Holven KB, Roos N, et al. Storage of vitamin A in extrahepatic stellate cells in normal rats. *J Lipid Res*. 1997;38:645–658.
40. Higashi N, Wake K, Sato M, Kojima N, Imai K, Senoo H. Degradation of extracellular matrix by extrahepatic stellate cells in the intestine of the lamprey, Lampetra japonica. *Anat Rec A Discov Mol Cell Evol Biol*. 2005;285:668–675.
41. Loo CK, Pereira TN, Pozniak KN, Ramsing M, Vogel I, Ramm GA. The development of hepatic stellate cells in normal and abnormal human fetuses - an immunohistochemical study. *Physiol Rep*. 2015;3:e12504.
42. Ichikawa S, Mucida D, Tyznik AJ, Kronenberg M, Cheroutre H. Hepatic stellate cells function as regulatory bystanders. *J Immunol*. 2011;186:5549–5555.
43. Dittadi R, Catozzi L, Gion M, et al. Comparison between western blotting, immunohistochemical and ELISA assay for p185neu quantitation in breast cancer specimens. *Anticancer Res*. 1993;13:1821–1824.
44. Kurien BT, Dorri Y, Dillon S, Dsouza A, Scofield RH. An overview of Western blotting for determining antibody specificities for immunohistochemistry. *Methods Mol Biol*. 2011;717:55–67.
45. Liang H, Crewther SG, Crewther DP, Junghans BM. Structural and elemental evidence for edema in the retina, retinal pigment epithelium, and choroid during recovery from experimentally induced myopia. *Invest Ophthalmol Vis Sci*. 2004;45:2463–2474.
46. Junghans BM, Crewther SG, Liang H, Crewther DP. A role for choroidal lymphatics during recovery from form deprivation myopia? *Optom Vis Sci*. 1999;76:796–803.
47. Burger NB, Stuurman KE, Kok E, et al. Involvement of neurons and retinoic acid in lymphatic development: new insights in increased nuchal translucency. *Prenatal Diag*. 2014;34:1312–1319.
48. Choi I, Lee S, Kyoung Chung H, et al. 9-cis retinoic acid promotes lymphangiogenesis and enhances lymphatic vessel regeneration: therapeutic implications of 9-cis retinoic acid for secondary lymphedema. *Circulation*. 2012;125:872–882.

Investigative Ophthalmology & Visual Science